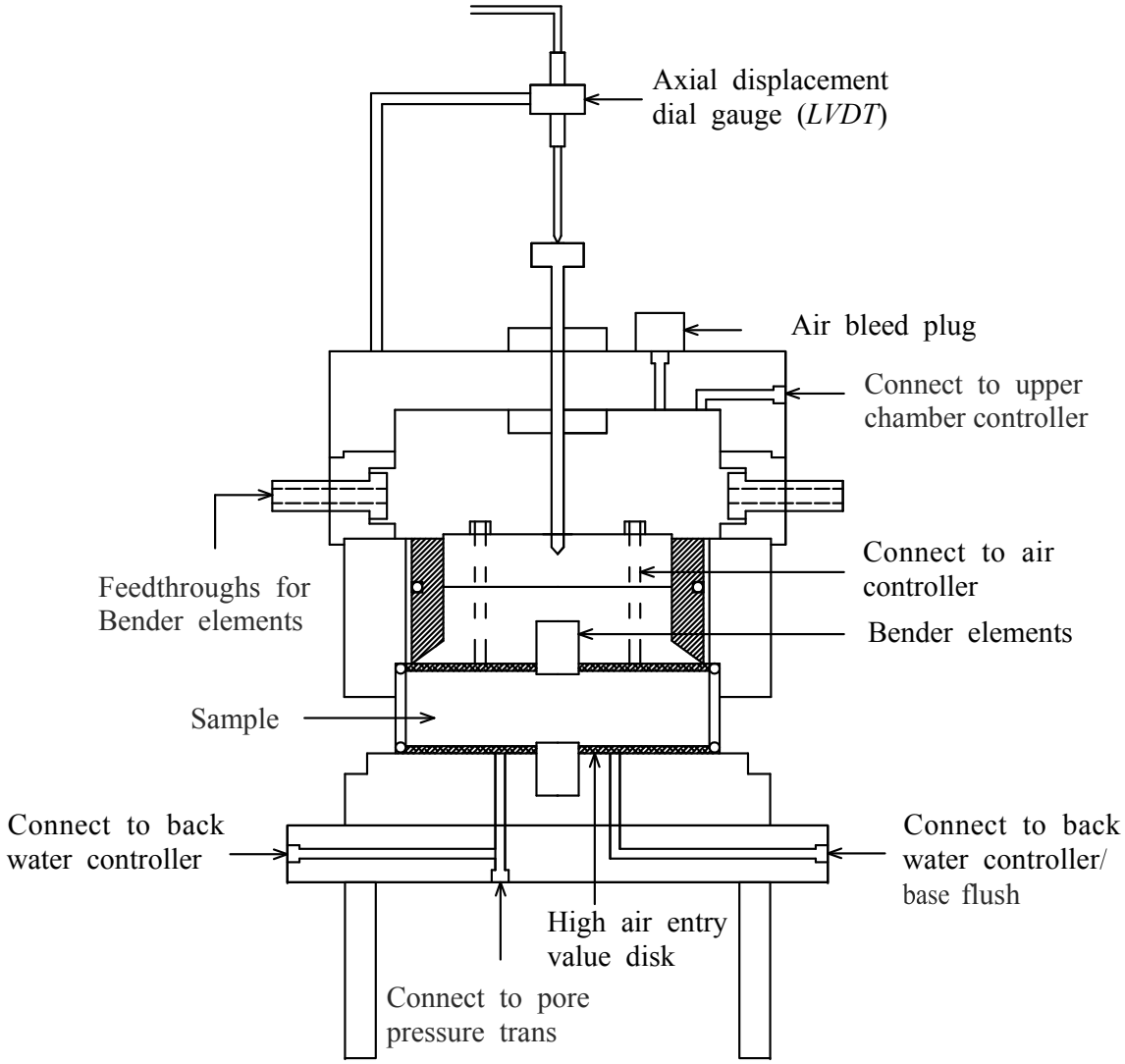
Axial displacement dial gauge (*LVDT*)
Air bleed plug
Connect to upper chamber controller
Feedthroughs for Bender elements
Connect to air controller
Bender elements
Sample
Connect to back water controller
Connect to back water controller/ base flush
High air entry value disk
Connect to pore pressure trans

a)

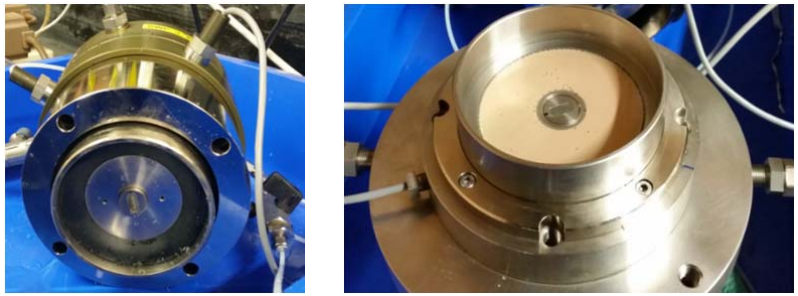

b) c)

Fig. 1. Modified Rowe cell apparatus with bender elements: a) schematic diagram of the Rowe cell setup; b) a photograph of the top loading system; and c) a photograph of the bottom pedestal

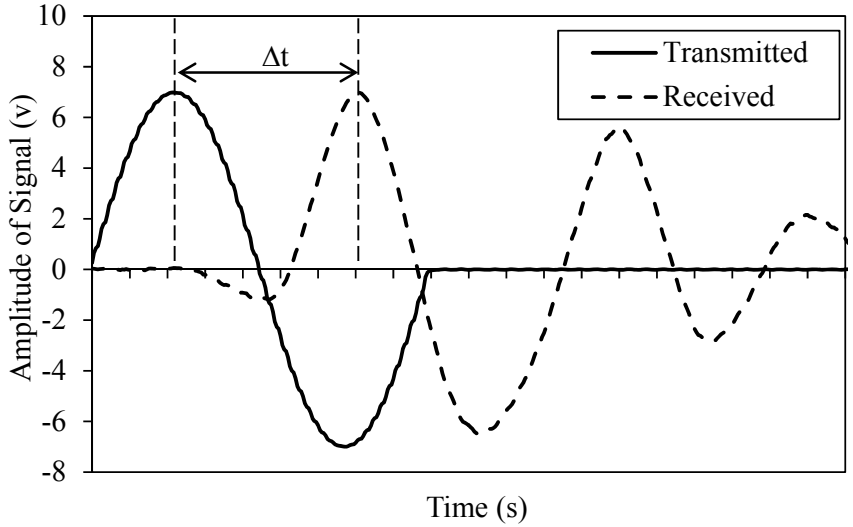

Fig. 2. Determination method for the shear wave propagation time in the Rowe cell equipped with two bender elements

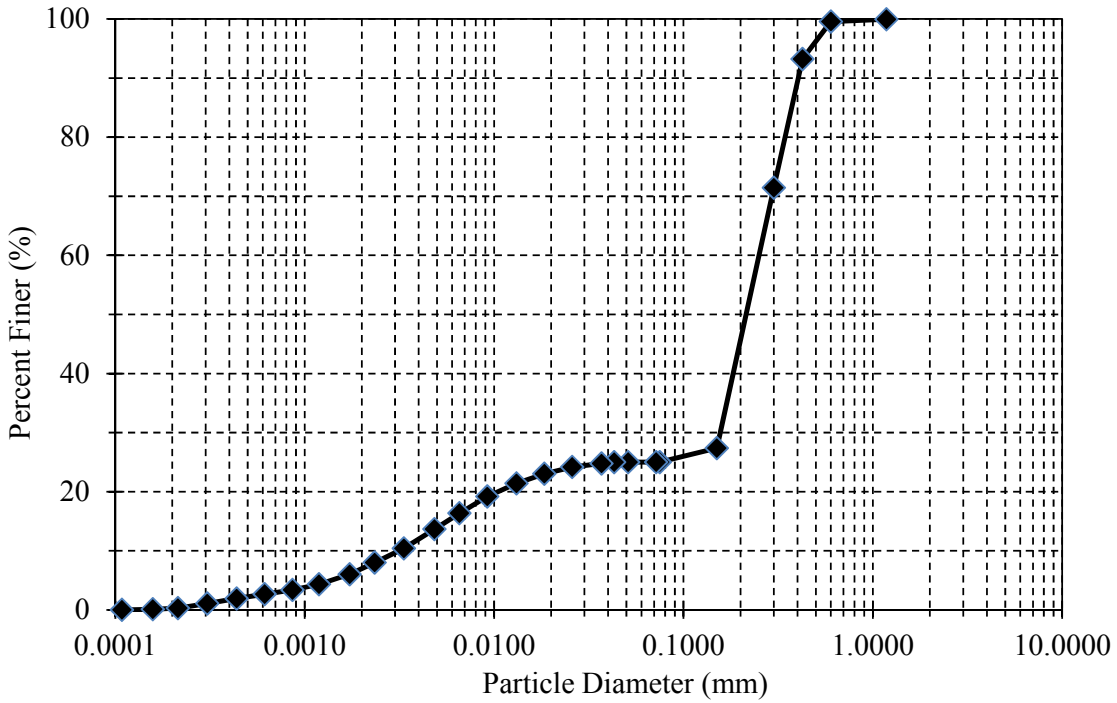

Fig. 3. Particle size distribution curve for the sand and kaolin mixture

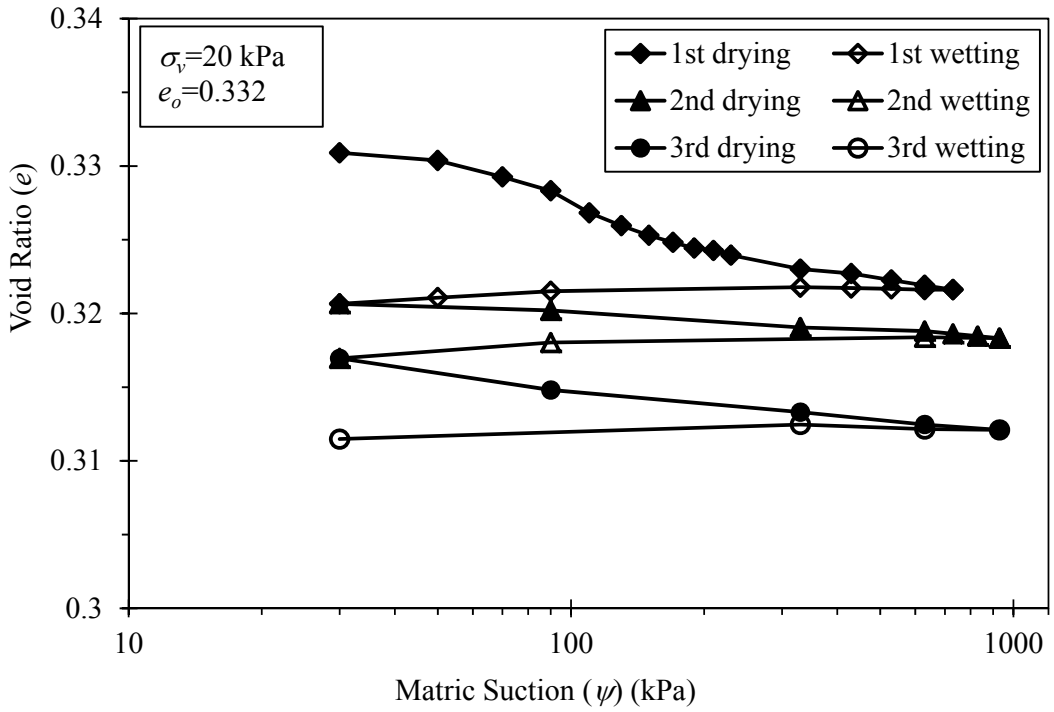

Fig. 4. Void ratio and matric suction (e-ψ) relationship during three drying-wetting cycles

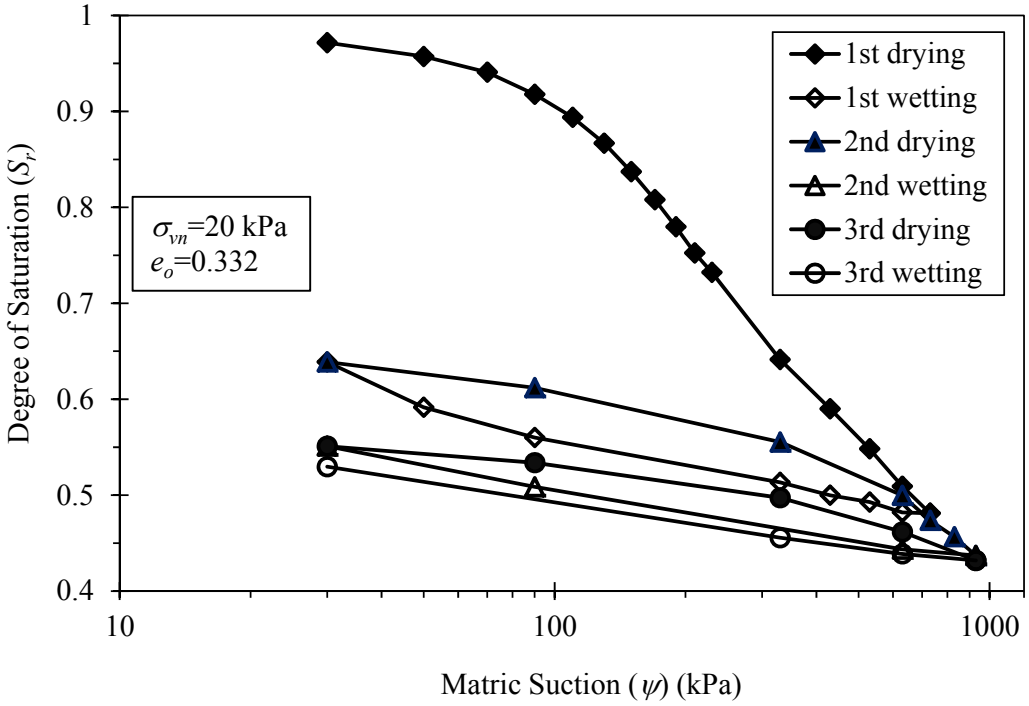

Fig. 5. Degree of saturation versus measured matric suctions (*SWCC)* in three drying-wetting cycles

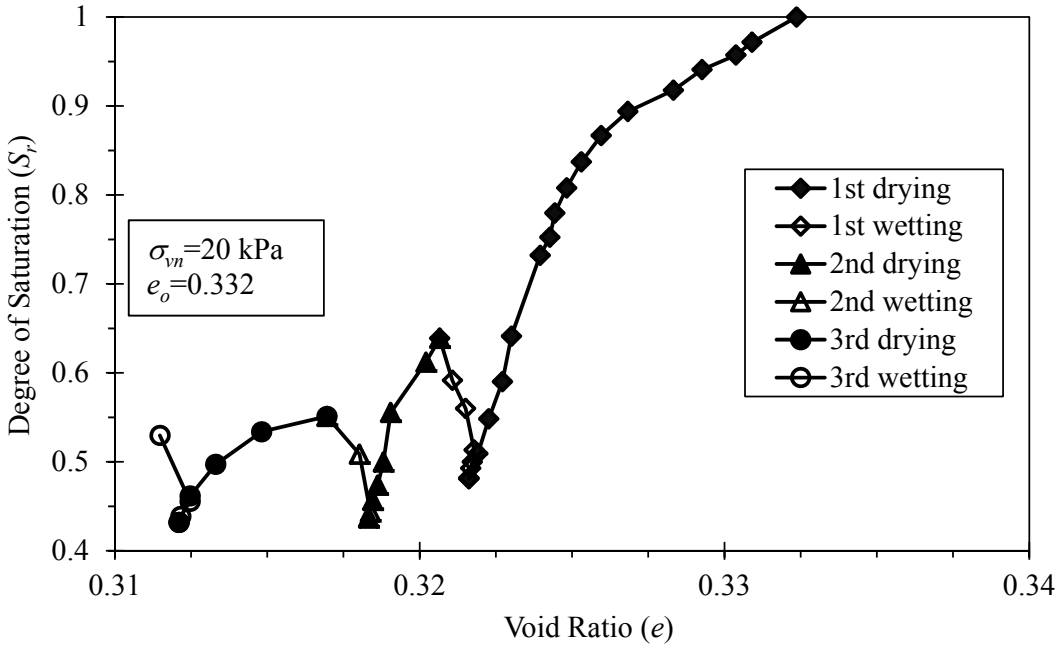

Fig. 6. S_r-e relationship during three drying-wetting cycles

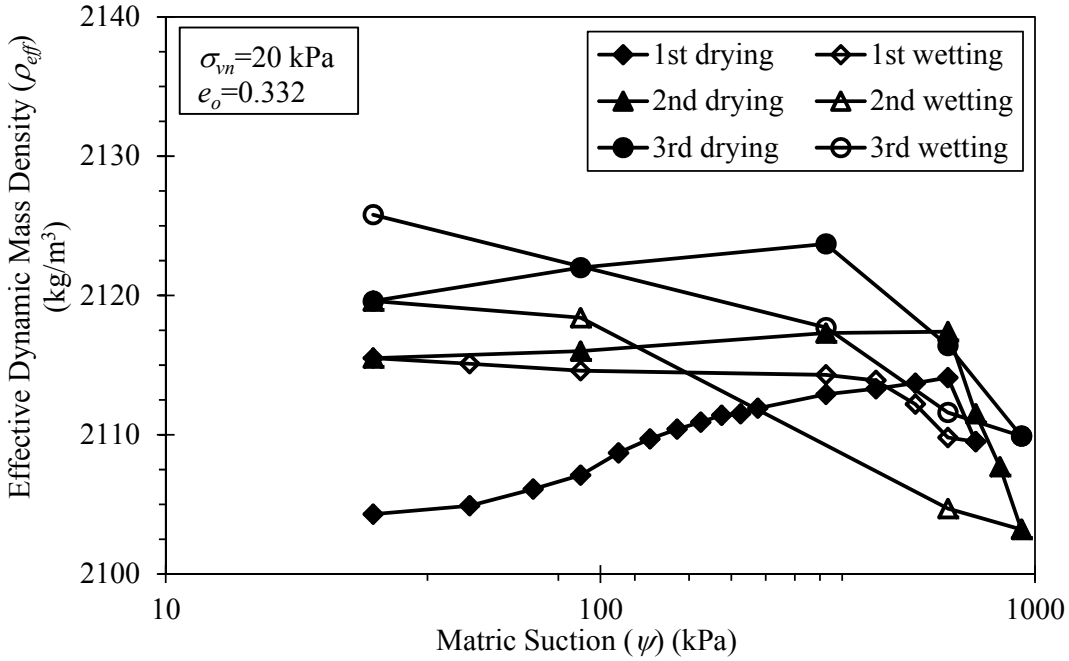

Fig. 7. ρ_{eff}-ψ relationship during three drying-wetting cycles

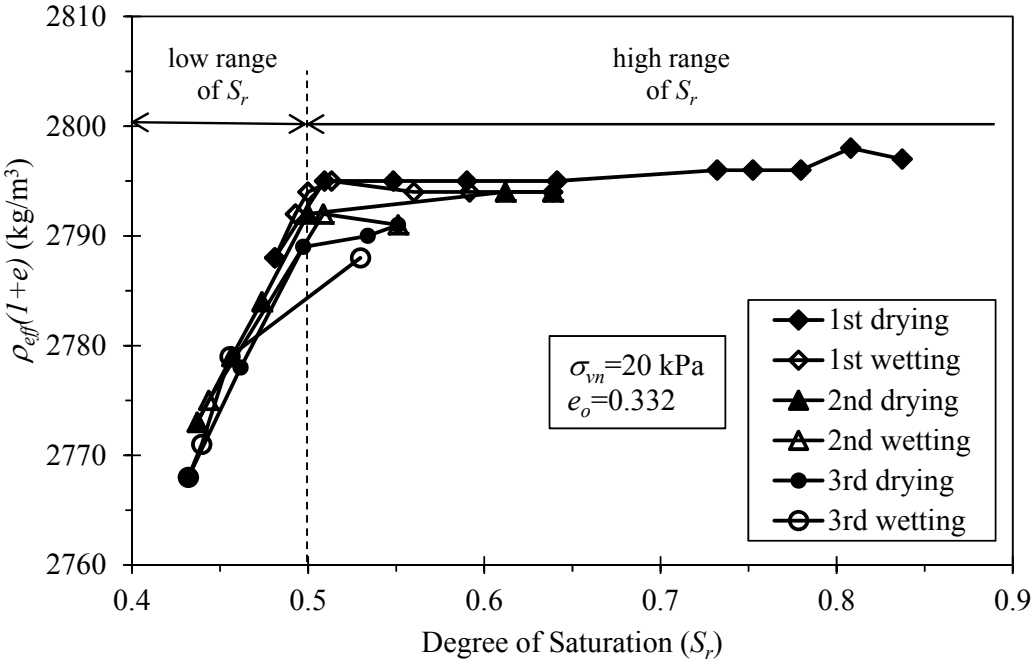

Fig. 8. S_r-$\rho_{eff}(1+e)$ relationship during three drying-wetting cycles

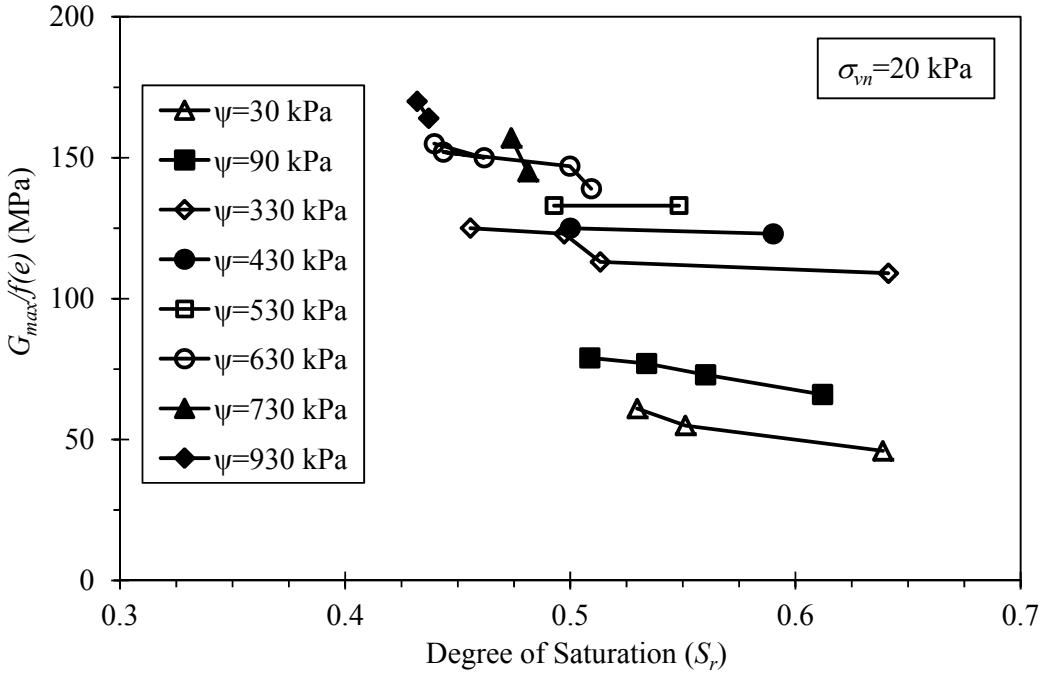

Fig. 9. $G_{max}/f(e)$- S_r relationship during three drying-wetting cycles

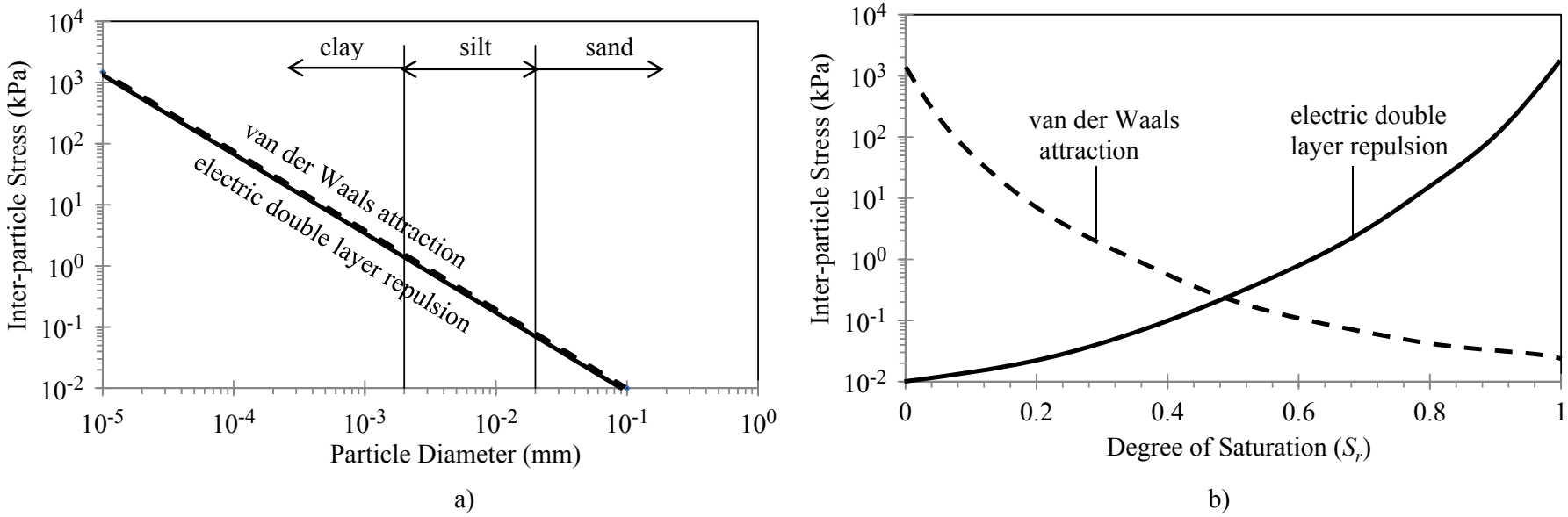

Fig. 10. Dependence of inter-particle stress generated by van der Waals and electric double layer forces on a) particle diameter (after Ingles 1962); and b) degree of saturation (adapted from Lu and Likos 2006)

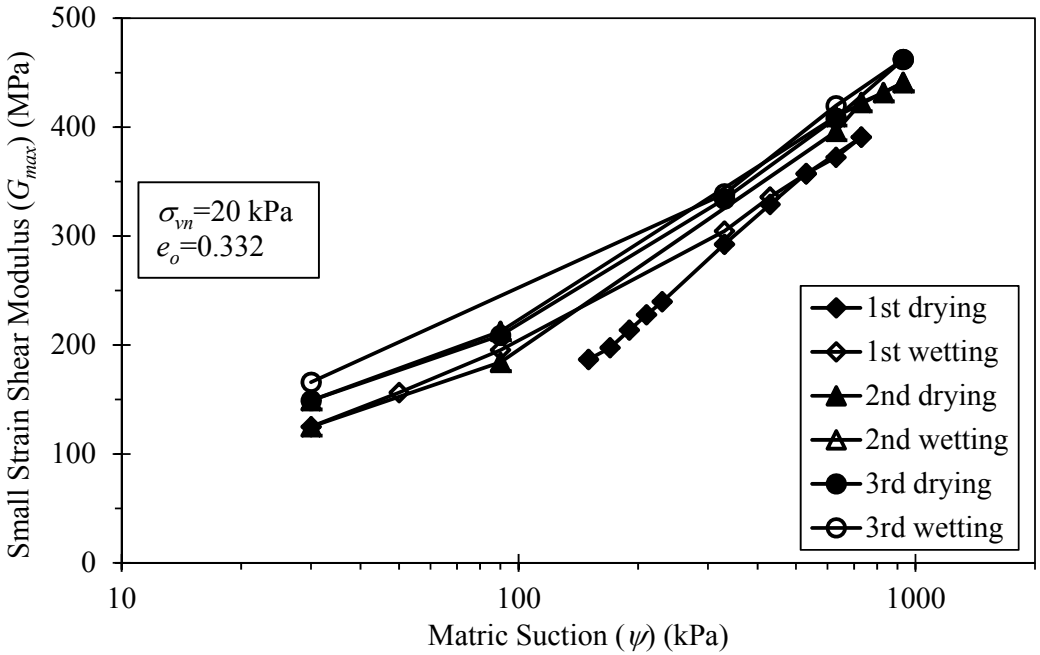

Fig. 11. G_{max}-ψ relationship during the three drying-wetting cycles

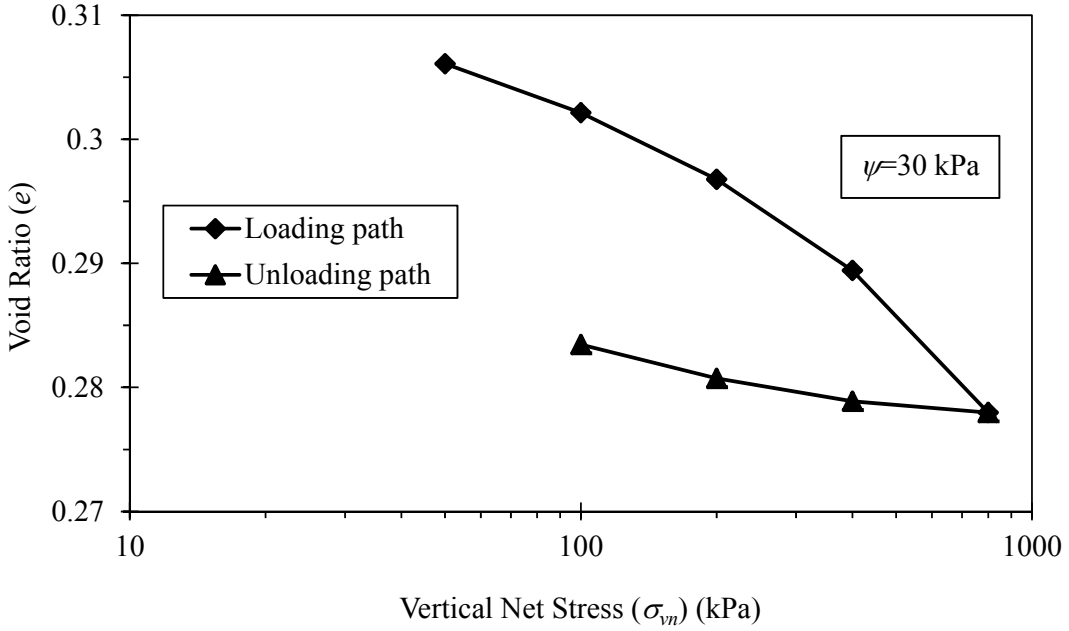

Fig. 12. σ_{vn}-e relationship in the loading-unloading cycle

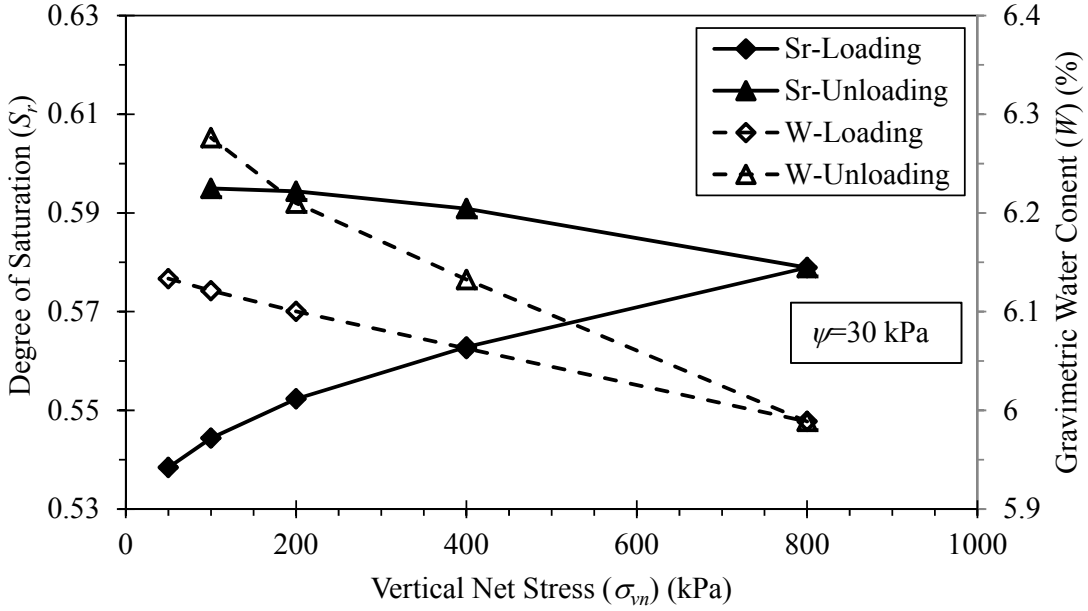

Fig. 13. Hydraulic hysteresis in a loading-unloading cycle

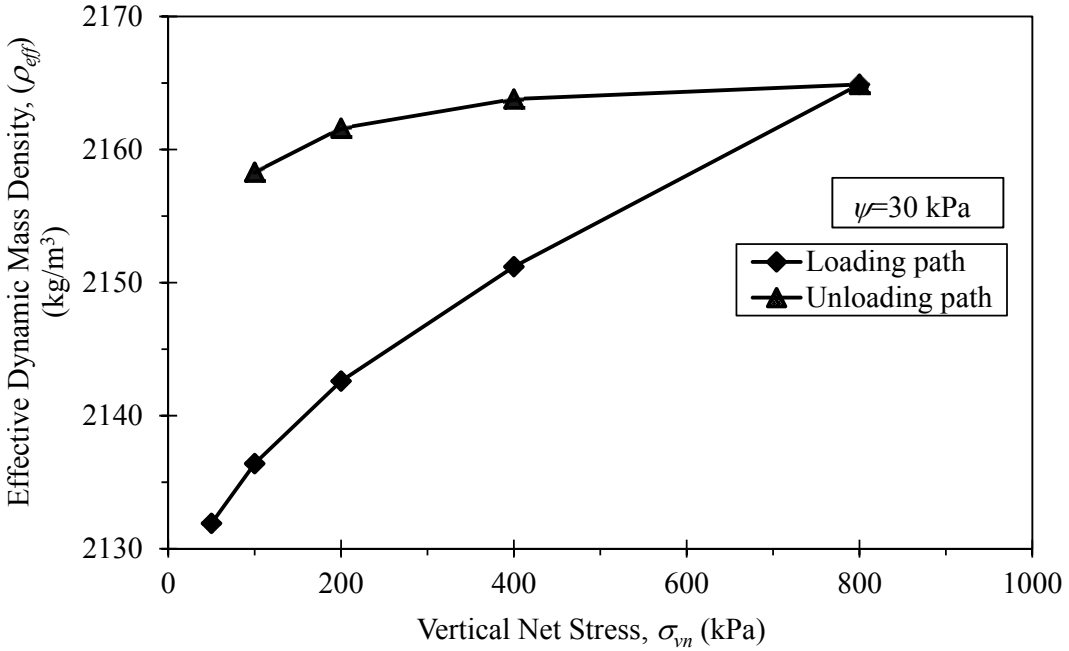

Fig. 14. σ_{vn}-ρ_{eff} relationship in a loading-unloading cycle

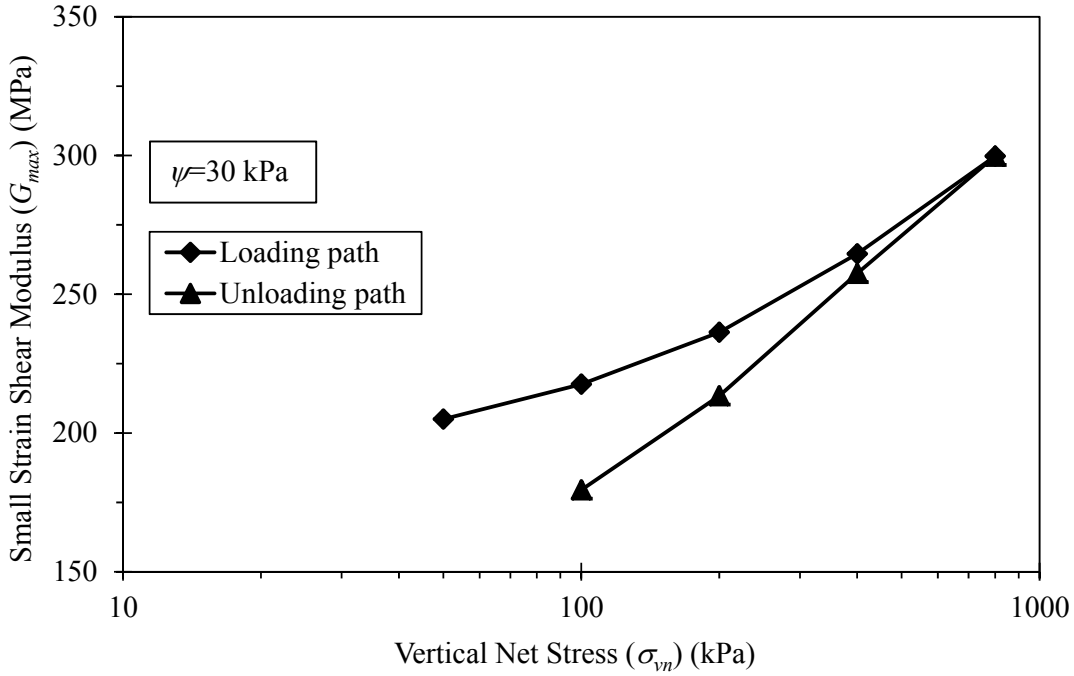

Fig. 15. σ_{vn}-G_{max} relationship in a loading-unloading cycle

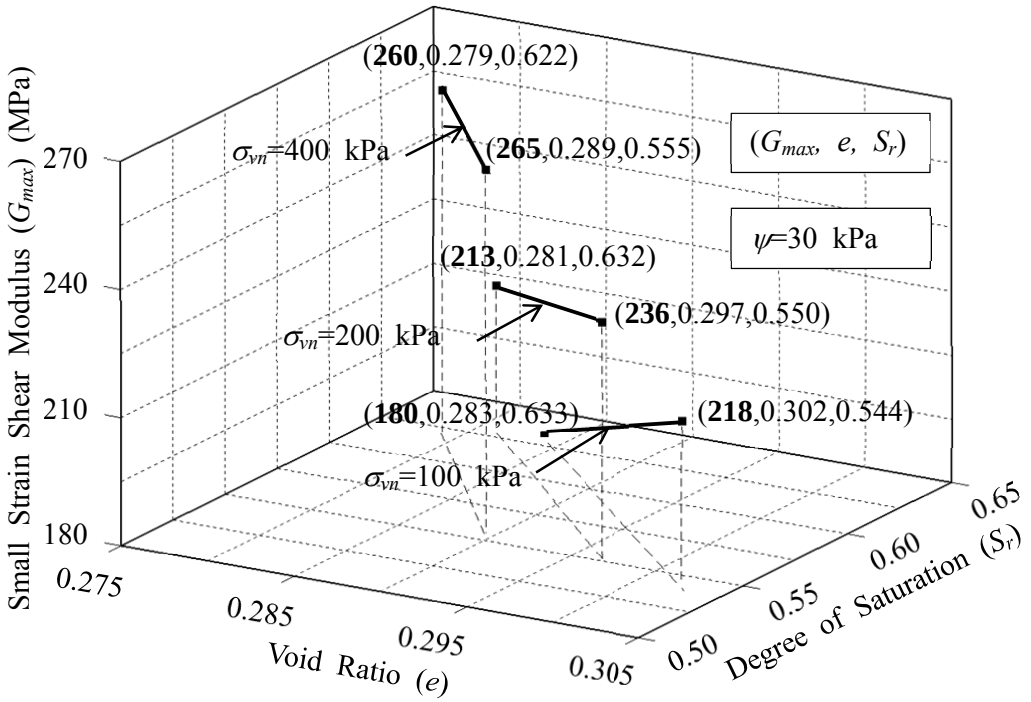

Fig. 16. Variation of G_{max} with void ratio and degree of saturation in the loading-unloading cycle

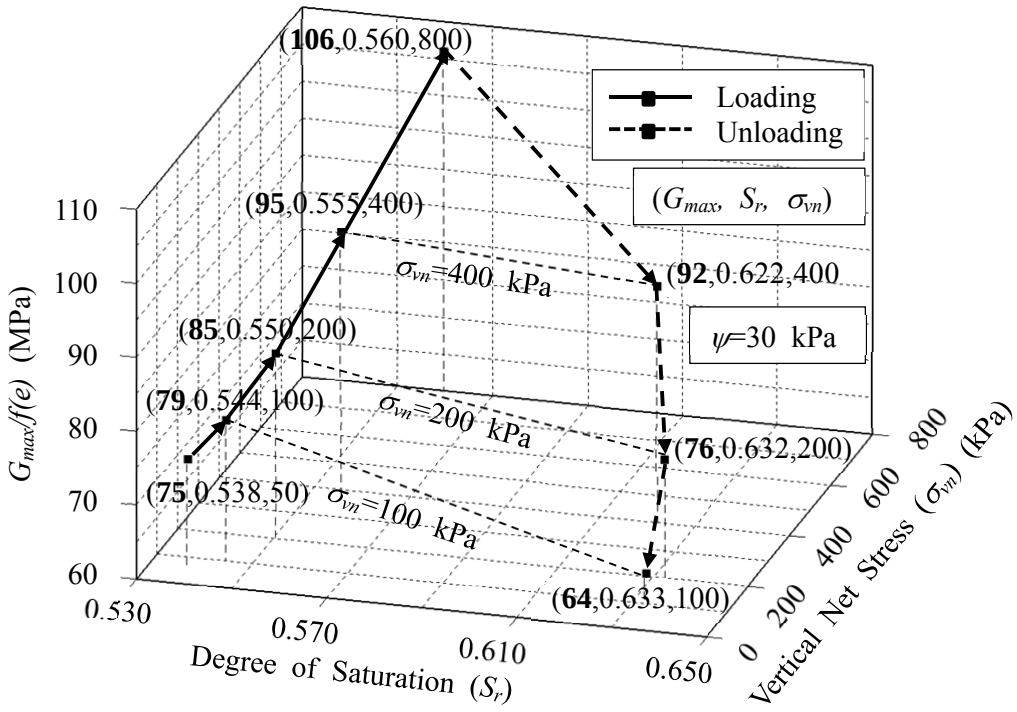

Fig. 17. Variation of $G_{max}/f(e)$ with vertical net stress and degree of saturation in the loading-unloading cycle

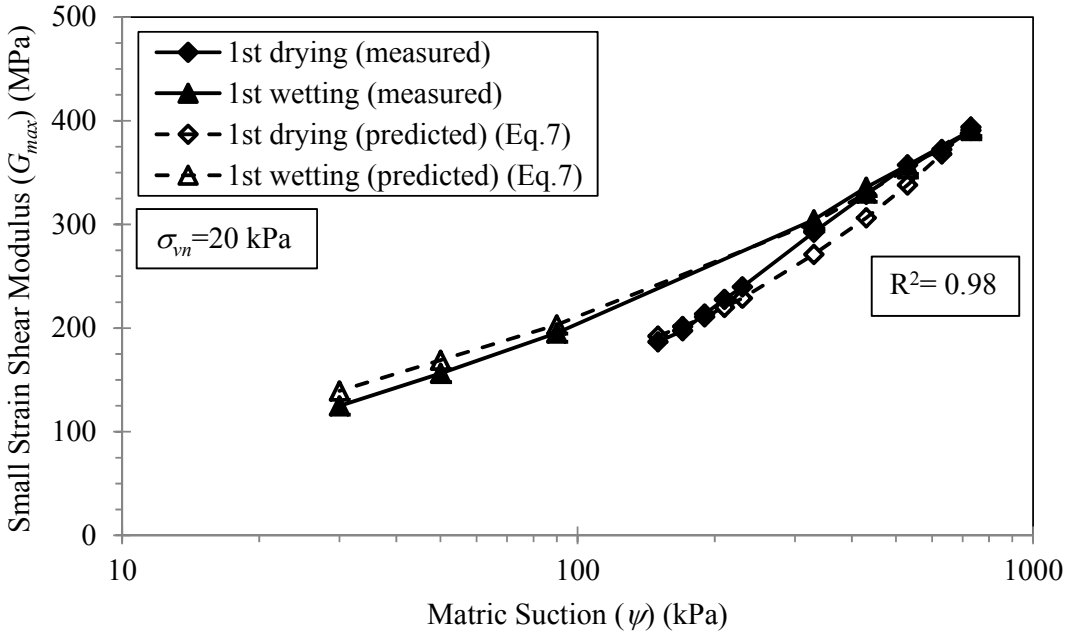
Small Strain Shear Modulus (G_{max}) (MPa)
500
400
300
200
100
0
10
100
1000
Matric Suction (ψ) (kPa)
1st drying (measured)
1st wetting (measured)
1st drying (predicted) (Eq.7)
1st wetting (predicted) (Eq.7)
σ_{vn}=20 kPa
R^2= 0.98

a)

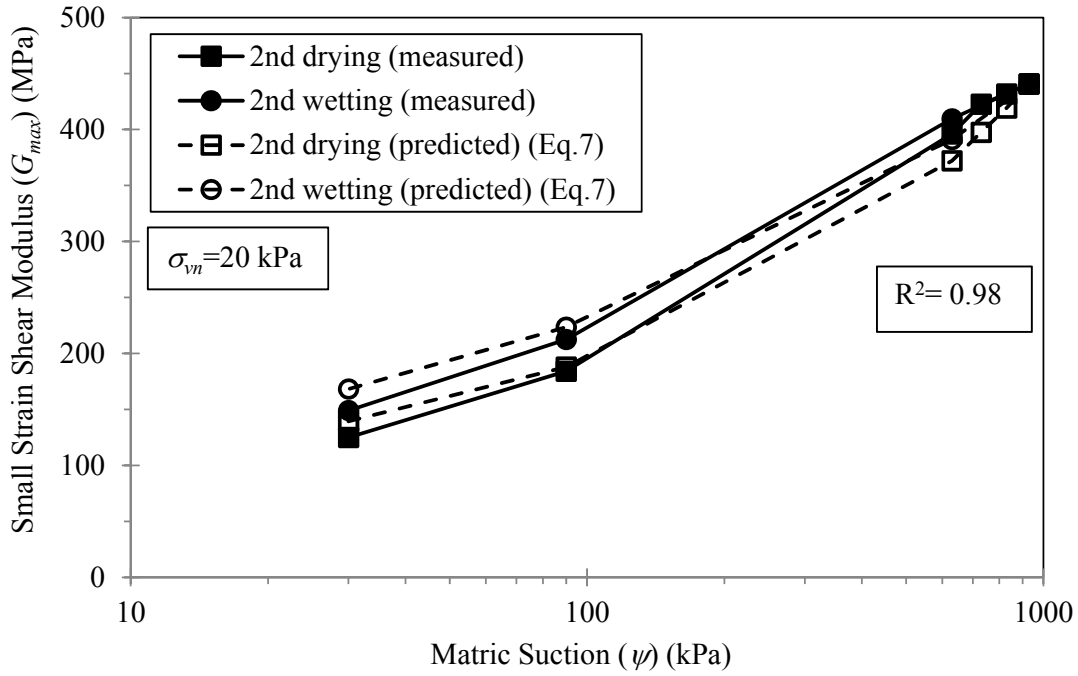
2nd drying (measured)
2nd wetting (measured)
2nd drying (predicted) (Eq.7)
2nd wetting (predicted) (Eq.7)
σ_{vn}=20 kPa
R^2= 0.98
Small Strain Shear Modulus (G_{max}) (MPa)
Matric Suction (ψ) (kPa)
500
400
300
200
100
0
10
100
1000
b)

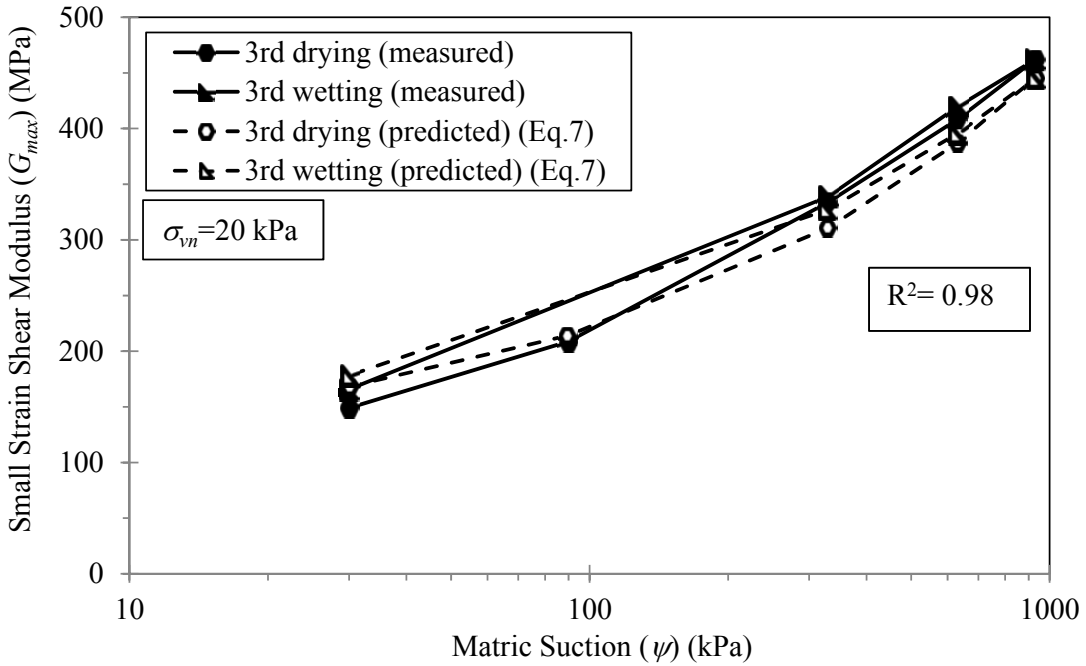
3rd drying (measured)
3rd wetting (measured)
3rd drying (predicted) (Eq.7)
3rd wetting (predicted) (Eq.7)
σ_{vn}=20 kPa
R^2= 0.98
Small Strain Shear Modulus (G_{max}) (MPa)
Matric Suction (ψ) (kPa)
500
400
300
200
100
0
10
100
1000

c)

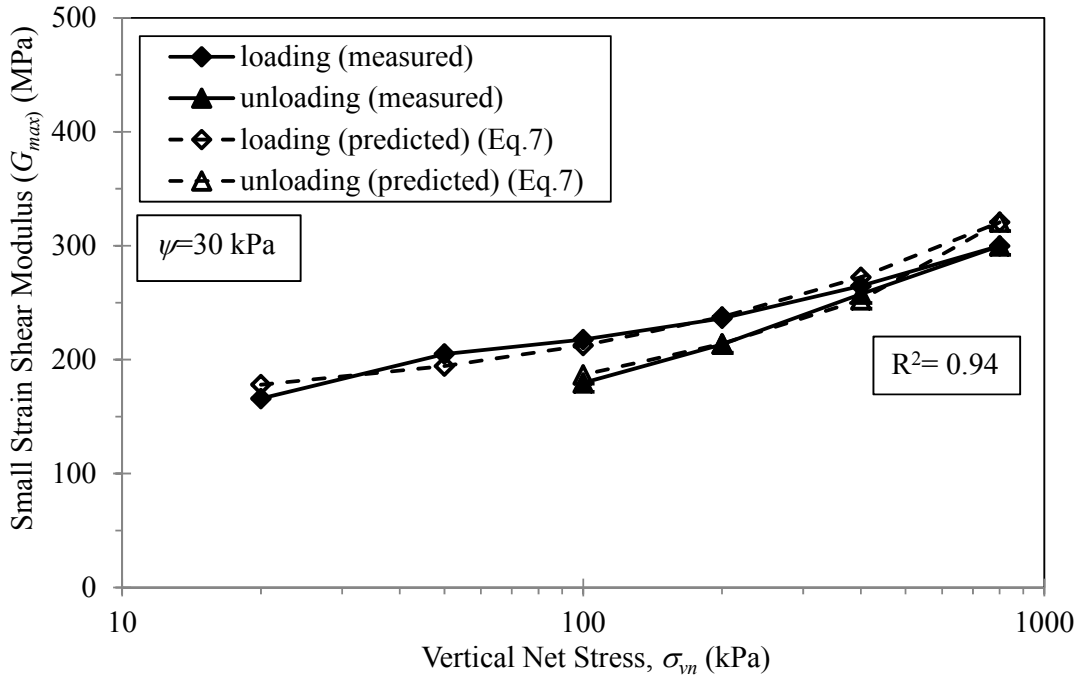

d)

Fig. 18. Measured and predicted G_{max} values during a) first; b) second; and c) third drying-wetting cycles; and d) loading-drying cycle

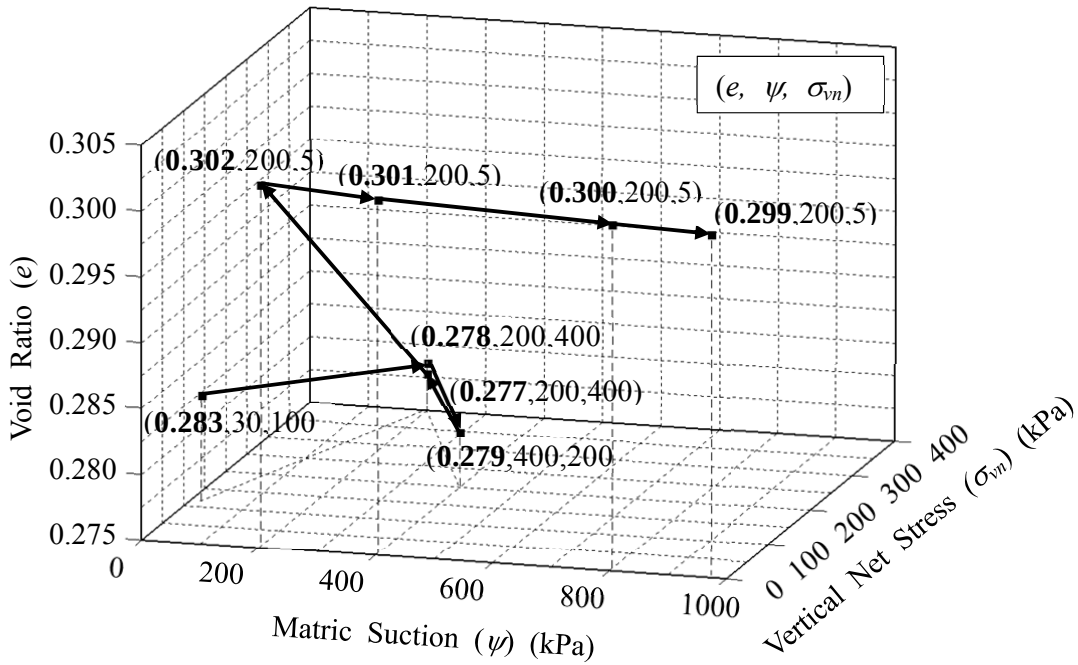
(e, ψ, σvn)
(0.302,200,5)
(0.301,200,5)
(0.300,200,5)
(0.299,200,5)
(0.278,200,400
(0.277,200,400)
(0.283,30,100
(0.279,400,200
Void Ratio (e)
0.305
0.300
0.295
0.290
0.285
0.280
0.275
0
200
400
600
800
1000
Matric Suction (ψ) (kPa)
0 100 200 300 400
Vertical Net Stress (σvn) (kPa)

a)

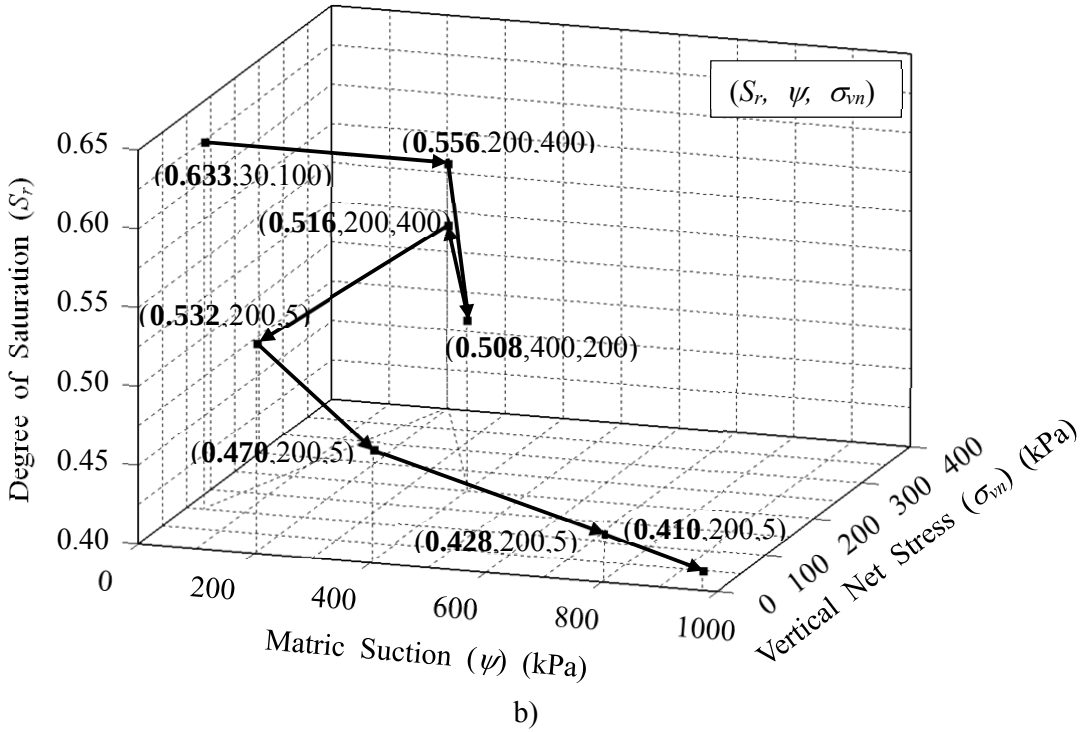

b)

Fig. 19. Variations of a) void ratio; and b) degree of saturation, during model test stages applying different matric suctions and net stresses

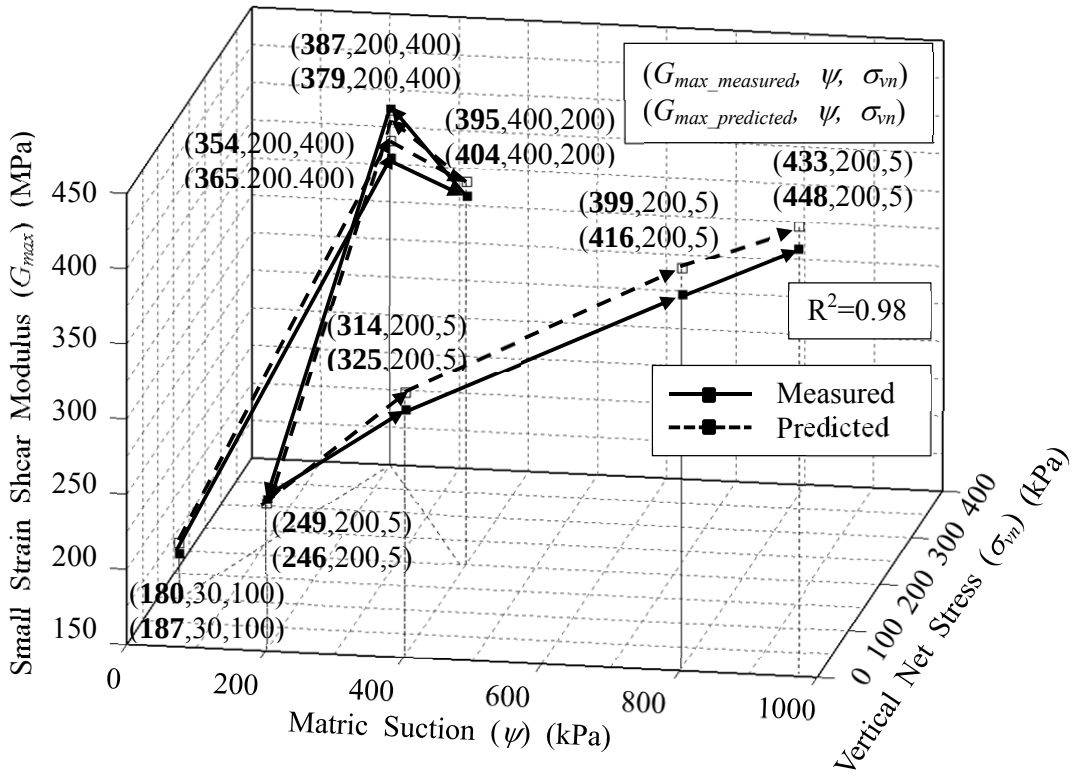

Fig. 20. Measured and predicted G_{max} values during model variation test stages

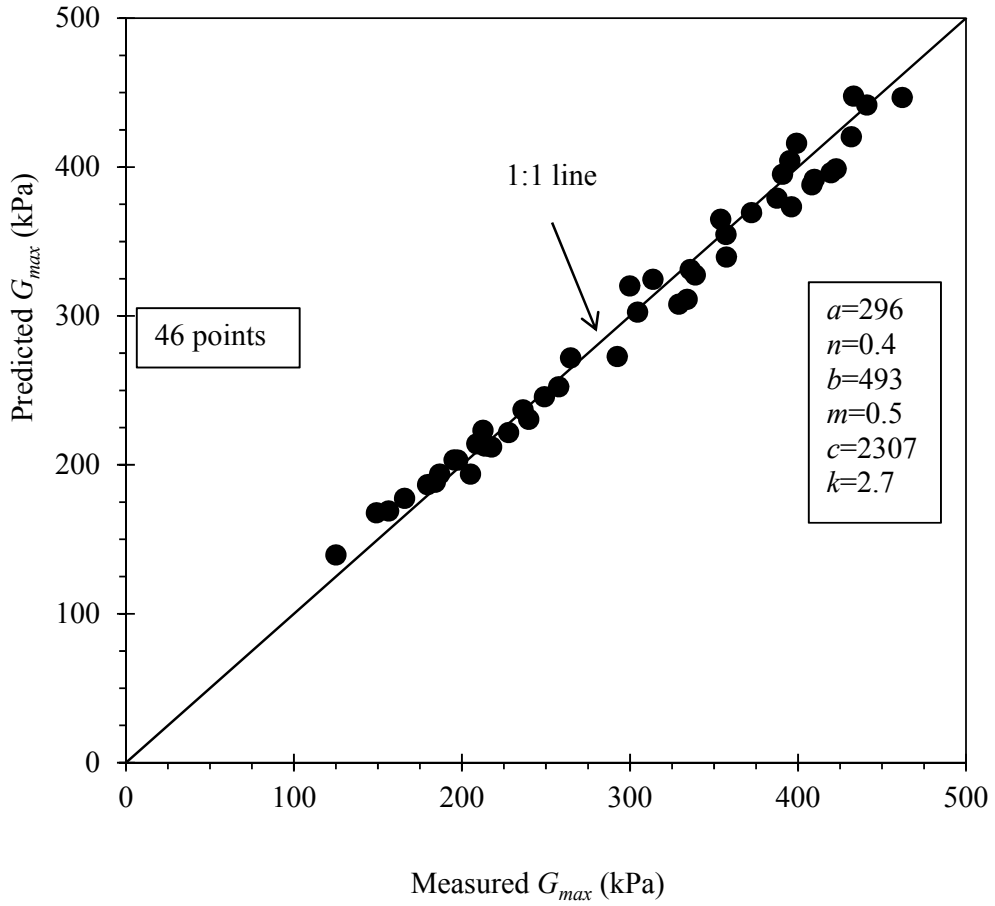

Fig. 21. The entire set of measured and predicted G_{max} values in this study

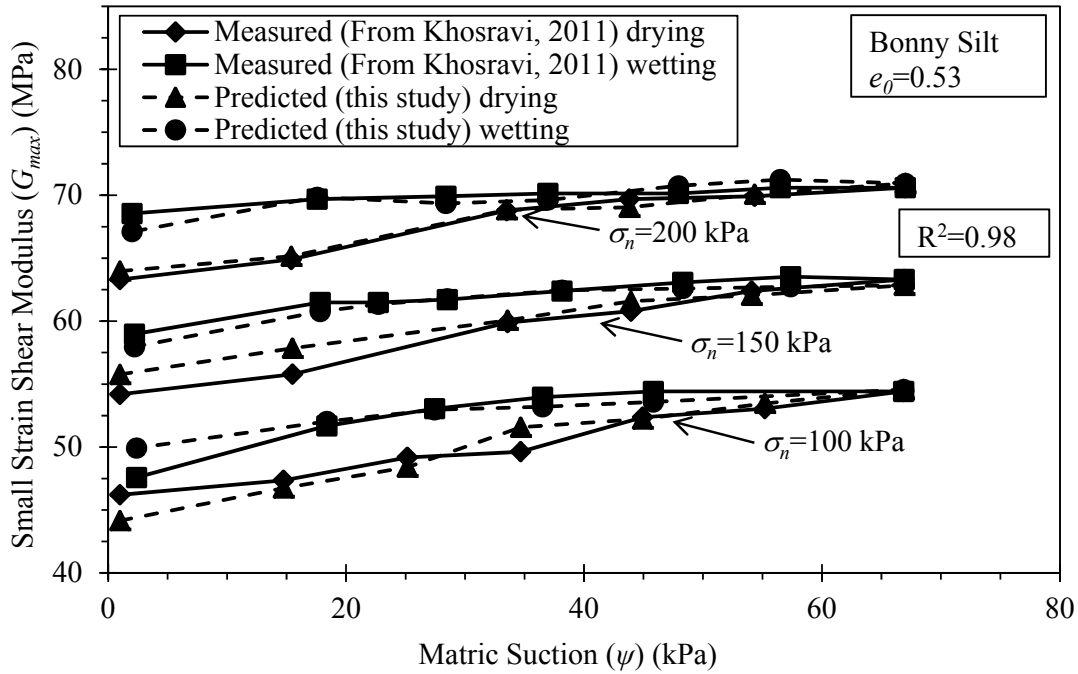
Measured (From Khosravi, 2011) drying
Measured (From Khosravi, 2011) wetting
Predicted (this study) drying
Predicted (this study) wetting
Bonny Silt
e_0=0.53
R^2=0.98
σ_n=200 kPa
σ_n=150 kPa
σ_n=100 kPa
Small Strain Shear Modulus (G_{max}) (MPa)
Matric Suction (ψ) (kPa)
40
50
60
70
80
0
20
40
60
80

a)

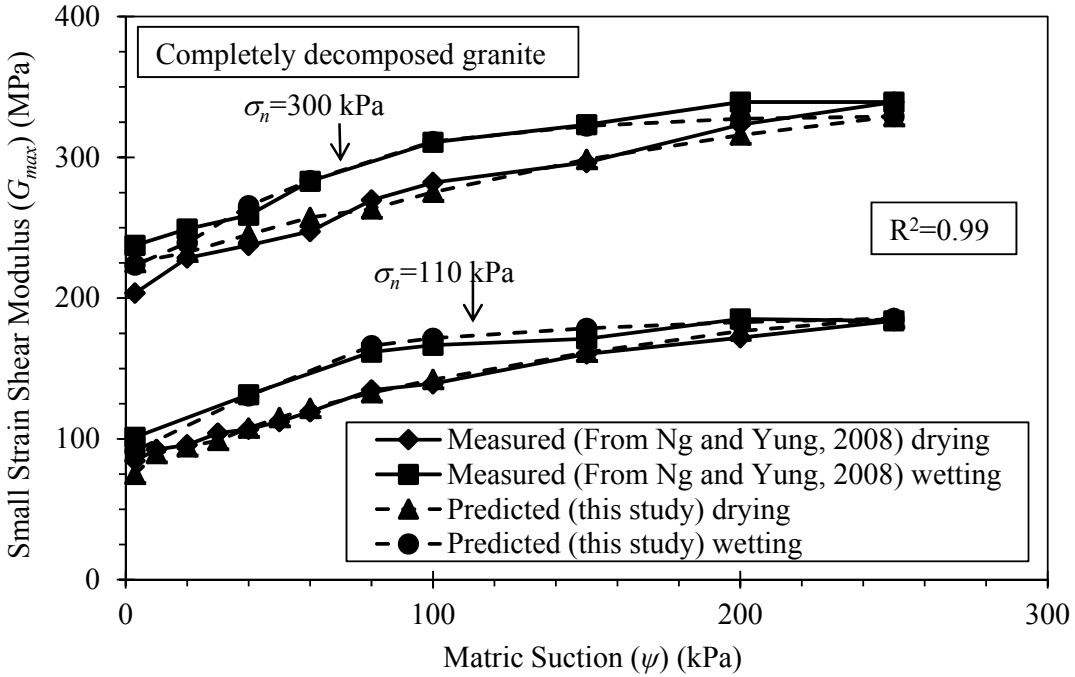
Completely decomposed granite
σ_n=300 kPa
σ_n=110 kPa
R^2=0.99
Measured (From Ng and Yung, 2008) drying
Measured (From Ng and Yung, 2008) wetting
Predicted (this study) drying
Predicted (this study) wetting
Small Strain Shear Modulus (G_{max}) (MPa)
Matric Suction (ψ) (kPa)
0
100
200
300
400

b)

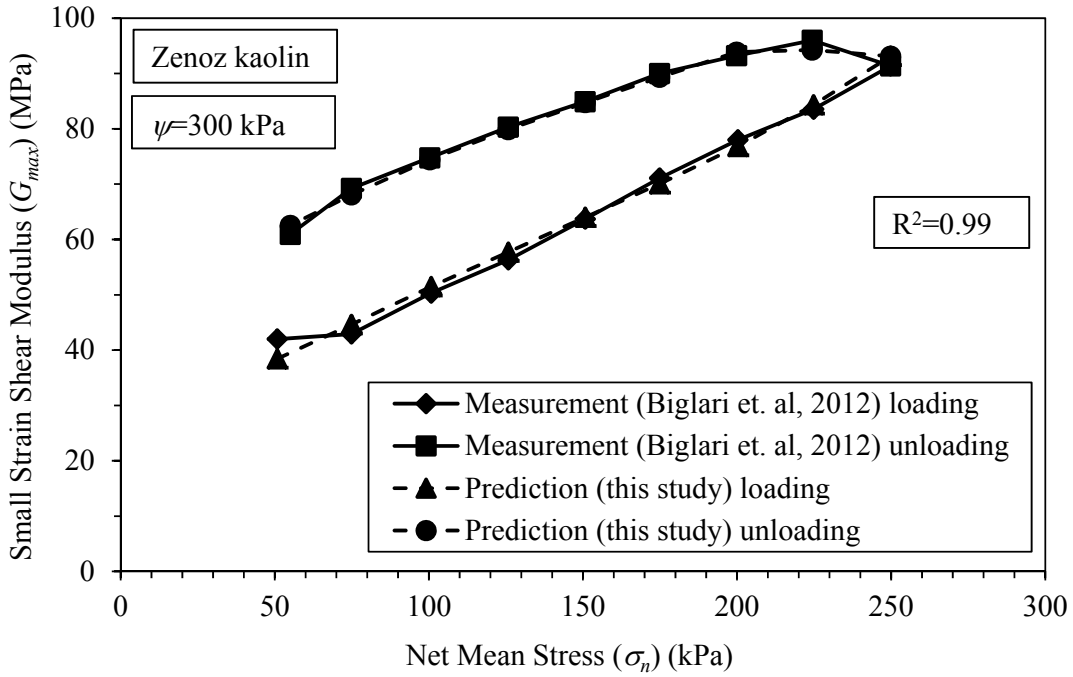

c)

Fig. 22. Prediction of G_{max} for a) Bonny Silt; and b) Completely decomposed granite during different drying-wetting cycles; and c) Zenoz kaolin during a loading-unloading cycle against net mean stress